Efficient, stable and accurate explicit recursive migration operators: A comparison

Jan Thorbecke[1]
Walter Rietveld[2]

A.1 Introduction

In homogeneous media the one-way extrapolation operator in the k_x-ω (wavenumber-frequency) domain is a simple analytical function. The advantage of computation in the k_x-ω domain is that the desired result is obtained by multiplication of the data with the operator. But simple multiplication in the k_x-ω domain rules out the possibility of applying a laterally varying operator. Another disadvantage is the numerical artefact in x due to undersampling in k_x. To allow laterally varying medium functions and less numerical artefacts a convolutional operator in the x-ω (space-frequency) domain should be used. When the spatial extrapolation operator is used in an explicit recursive depth migration algorithm it must be calculated in an optimum way to obtain reliable and stable results.

There are several ways to obtain a spatial convolution operator. For homogeneous media one usually starts with the exact analytical expression in the k_x-ω domain and transforms this operator back to the spatial domain. In recent years many methods have been developed to do this transformation in an efficient and optimum way. For the one-way extrapolation operator Hol-

1. E-mail: jan@delphi.tn.tudelft.nl
2. E-mail: walter@delphi.tn.tudelft.nl

berg (1988), Blacquiére (1989), Hale (1990) and Nautiyal et al. (1993) have proposed methods to arrive at spatial operators which are unconditionally stable in a recursive extrapolation scheme. In DELPHI Volume IV, Appendix D (1993) an alternative method is presented for an efficient and controlled transformation back to the spatial domain. This method can be used to calculate extrapolation operators which should be stable and accurate in a recursive depth migration algorithm. First some examples of extrapolation operators for homogeneous media are given. The theoretical derivation for the proposed numerical optimization scheme was already given in Appendix D of the DELPHI Volume IV (1993). The proposed method is compared with other numerical optimization methods and finally some results of recursive depth migration, in acoustic media with the optimized extrapolation operators, are given.

A.2 Analytical space-frequency operators

In the k_x-ω domain the extrapolation operator is, for a two-dimensional medium, given by the familiar phase-shift operator:

$$\tilde{W}(k_x) = \exp(-jk_z\Delta z), \tag{A.1}$$

with

$$k_z = \sqrt{k^2 - k_x^2}, \tag{A.2}$$

in which k_x denotes the wavenumber, Δz the extrapolation depth and k is defined as ω/c, with c the propagation velocity of the medium and ω the angular frequency. For wavenumber values larger than k, the wavefield becomes evanescent. The analytical inverse Fourier transform of equation (A.1) is a scaled Hankel function (see Berkhout, 1985):

$$W(x) = \frac{-jk\Delta z}{2\sqrt{x^2 + \Delta z^2}} H_1^{(2)}\left(k\sqrt{x^2 + \Delta z^2}\right). \tag{A.3}$$

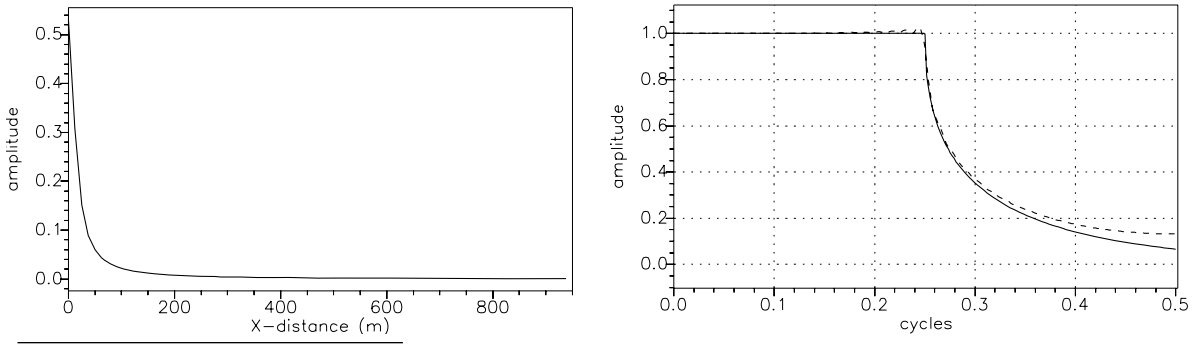

Figure A.1: *Analytical spatial extrapolation operator (left) and its wavenumber spectrum (right). The dashed line is related to the truncated analytical operator (151 points) and the solid line to the exact operator. Note the excellent agreement: for 151 samples the truncation error is negligible.*

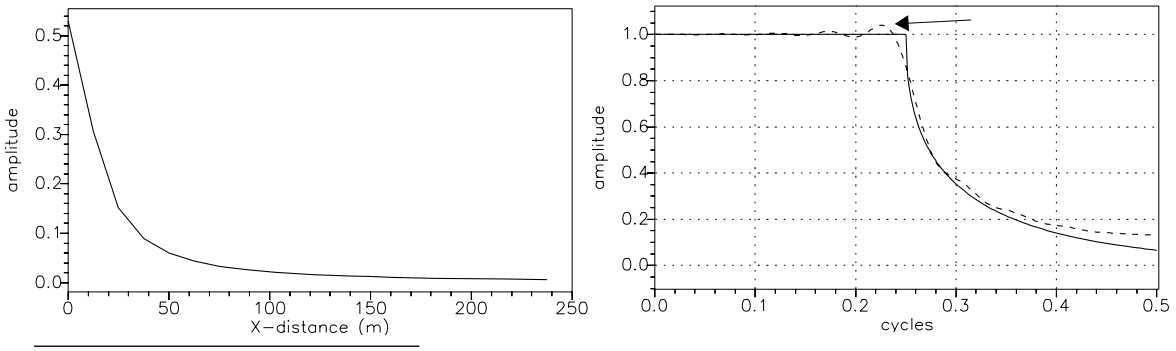

Figure A.2: *Same illustration as in Figure A.1, but now the number of samples is reduced to 39 points. Note the unacceptable truncation effect which is indicated by the arrow in the right picture.*

In Figure A.1 the amplitude of equation (A.3) is given as function of x. The amplitude of the wavenumber spectrum of this truncated function (dashed line) is displayed together with the phase shift operator $\tilde{W}(k_x)$ (solid line). We have used the same parameters as Hale (1991) and Nautiyal et al. (1993); $\Delta z = \Delta x = 12.5$ m, $\omega = 40\pi$ radians/s, 512 wavenumbers and $c = 1000$ m/s. The horizontal axes in Figure A.1 represents normalized wavenumber cycles ($n\pi/N$, radians per sample in the x direction; i.e. for 0.25 the angle of wavenumber k is 90^o and for 0.1 the angle is 36^o). The number of samples in the spatial domain is chosen at 151. In the Figures shown in this appendix only the positive values for k_x and x are displayed because of the symmetry of the operators, so in Figure A.1 only 76 x-positions are shown. From Figure A.1 it can be seen that the Hankel function is a long operator and is therefore not very well suited for recursive depth extrapolation. From a computational point of view long spatial operators are not desired because multiplication in the wavenumber-frequency domain is replaced by a convolution in the space-frequency domain. Further, the locally homogeneous assumption in inhomogeneous media is for a long operator pushed to its limits. If we truncate the Hankel function to a more suitable number of points (for example 39 points) then we see that the wavenumber spectrum is not stable for wavenumbers near to k (see Figure A.2).

A solution to this truncation problem is given by Nautiyal et al. (1993). Their main concern was stability. They argued that accuracy is important for any numerical method but stability is crucial because an unstable, accurate method is even less useful than a stable but inaccurate one. They propose to taper the spatial wavelet with a Gaussian taper (to guarantee a stable extrapolation operator). As an example we can apply a Gaussian taper to the operator shown in Figure A.2. The chosen Gaussian taper decays from a value of 1 at $x = 0$ to a value of $\cos^2(\pi N/(2(N+1))$ at $x = dx*(N-1)/2$, with $N = 39$ (after Nautiyal et al. , 1993). The results are shown in Figure A.3. Note that the Hankel function is designed as the inverse Fourier transform of the phase shift operator and not as the Hankel function directly in the spatial domain. In this way aliasing of the higher wavenumbers in the wavenumber domain is avoided. We see that the wavenumber spectrum is now unconditionally stable for all wavenumbers, but the accuracy is reduced for higher wavenumbers. Another disadvantage is that the effective wavenumber band, in which the filtered analytical operators work, is not under control. It will be shown that control over the bandwidth of the spatial operator is essential for a desired operator functionality.

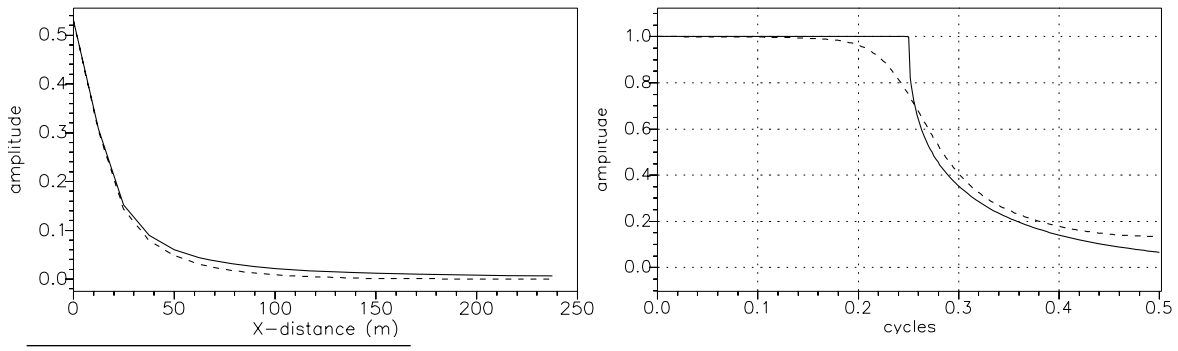

Figure A.3: *Same illustration as in Figure A.2, but now a spatial Gaussian taper is included as well. Note the unacceptable amplitude decay at high propagation angles.*

Another way to obtain stable extrapolation operators is to start in the wavenumber domain and transform the wavenumber expression back to the space domain. There are many ways to do this transformation in a desired way. In the next section we will discuss three different transformation methods. Note again that when the spatial convolution operator, obtained from the transformed operator in the k_x-ω domain, is applied in inhomogeneous media we must assume a local homogeneous medium around the center point of the convolution operator.

A.3 From wavenumber to spatial operators

The most straightforward way to obtain a spatial convolution operator from the expression in the k_x-ω domain is to calculate the inverse Fourier transform of this expression in the space - frequency domain and truncate this operator to a desired convolution length. Unfortunately this simple method is not stable for all wavenumbers and can therefore not be used in a recursive migration scheme.

Another way is to design a k_x-ω operator in such a way that the inverse Fourier transform is short so that truncation does not significantly effect the spectrum of interest. This method is developed by Blacquière (1989). The trick in this method is that the phase of the phase shift operator is slowly smoothing down for angles larger than the design angle. The extrapolation operator is obtained by taking the exponent of this smoothed phase $\exp(-jk\phi(k_x))$. This function is filtered with respect to the maximum design angle. In this way the amplitude spectrum of the operator is not decaying with the exponentially slope known from the phase shift operator but is determined by the wavenumber filter (see Figure A.4a right hand-side). It is known from Fourier analysis that large amplitude derivatives in the wavenumber domain as well as large phase derivatives give rise to large operator lengths (Blacquière, 1989). So the wavenumber filter should keep the operator as smooth as possible to make a short spatial operator, for example filtering with a cosine taper to $\pi/\Delta x$. The unfiltered operator is shown in the right-hand side of Figure A.4a for an maximum design angle of 70^o. We see that this operator has unit amplitude for all wavenumbers and the phase, shown in the left-hand side, is smoothly deviating from the exact operator (the dotted line) for angles greater than the design angle. In Figure A.4b the trun-

a) Smoothed design of extrapolation operator in wavenumber phase (left) and amplitude spectrum (right).

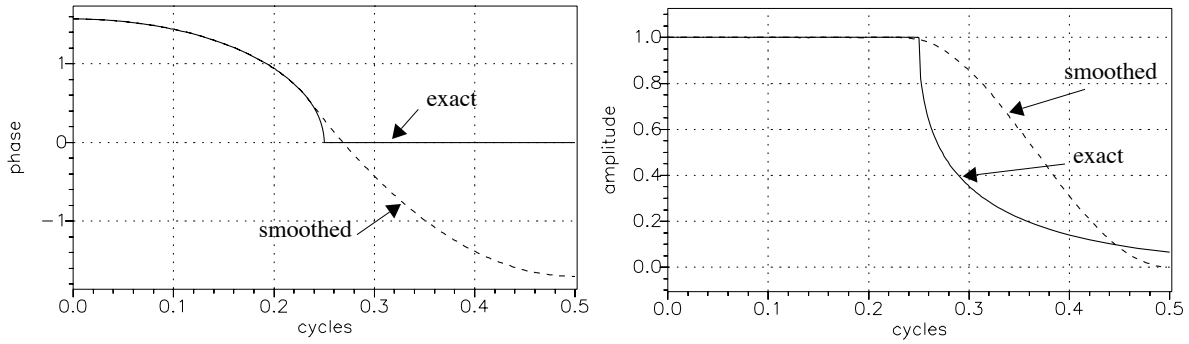

b) Truncated operator of 39 points (left) and the wavenumber amplitude spectrum (right).

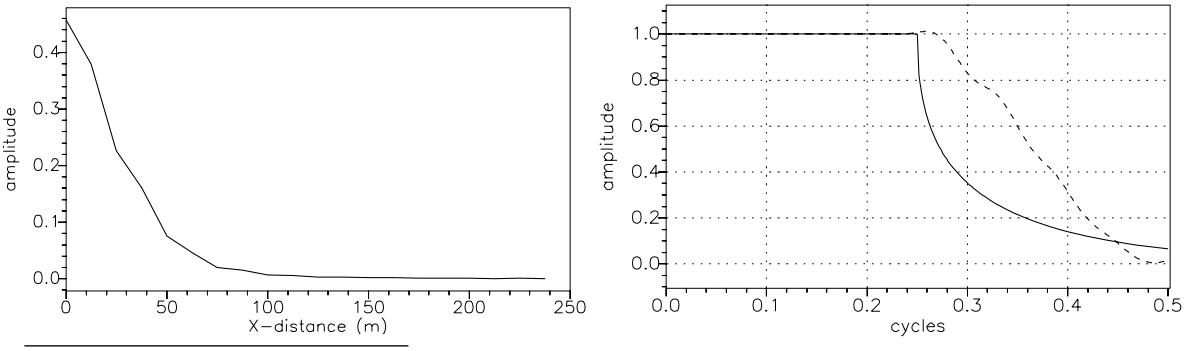

Figure A.4: *Due to the small derivatives in the wavenumber domain the artefacts for truncated operators remains small.*

cated operator (39 points) and the wavenumber spectrum is shown. In comparison with Figure A.2 we see that this operator is stable for all wavenumbers of interest.

The third way that will be discussed in this Appendix is the optimization procedure described in DELPHI Volume IV, Appendix D (1993). In this weighted least-square procedure the weighting function is defined in such a way that the wavenumbers of interest are given a high weight. The wavenumbers which are not of interest are 'abused' to make the operator as good as possible (given a low weight factor). The method described by Hale (1991) also uses some part of the wavenumber spectrum (degrees of freedom) to force the amplitude spectrum to zero in the evanescent region. The weighted least squares method we use only demands a stable

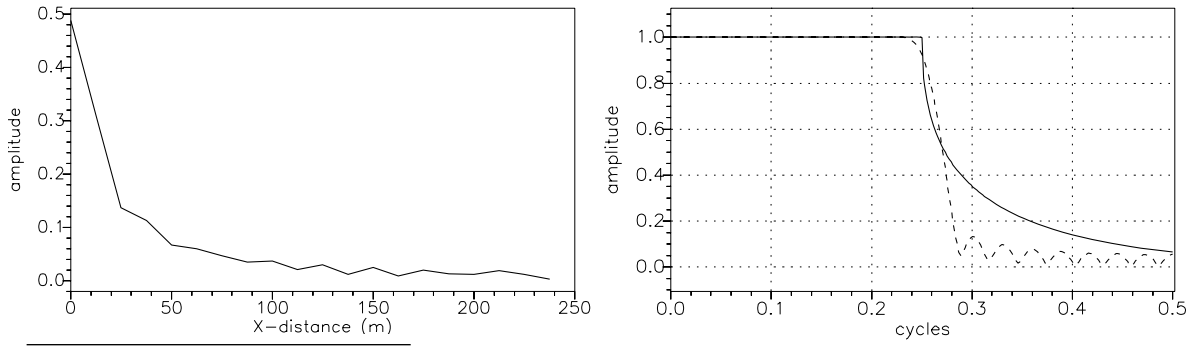

Figure A.5: *Weighted least square operator of 39 points (left) and its wavenumber spectrum (right). The solid line is related to the spectrum of the optimized operator and the dashed line to the exact operator. Note the perfect match in the propagating part of the wavenumber domain.*

(amplitude < 1) behaviour of the wavenumbers in the evanescent region. The used weighting function is a simple block with weight one inside the range of angles of interest and a small value (1e-5) outside this band. How these optimized operators, with the same parameters as before, behave is shown in Figure A.5. The spatial operator has a less 'smooth' character but the wavenumber spectrum is stable and accurate for all wavenumbers. Note the special character of the evanescent part of the wavenumber spectrum. It is not smoothing down but varying. This can be better observed if we look at a k_x-ω picture of the operators in Figure A.6 again with the same parameters and the frequency varying from 0 to 60 Hz. Holberg (1988) used a same presentation and argued that when the phase and amplitude errors are oscillating functions of the wavenumber these errors will not accumulate at the maximum possible rate when waves are propagated through inhomogeneous media. So the obtained operators could be used in a recursive migration scheme. In the calculation done to obtain Figure A.6 we have searched for a suitable weighting function in such a way that the amplitude of the wavenumber operator is ensured to be < 1.0004.

The most advanced and complicated method to compute a spatial convolution operator is by non-linear optimization. Holberg (1988) and Blacquière (1989) have both used a non-linear optimization method to compute stable and accurate operators. In non-linear optimization methods an objective function and a constraint function have to be defined. The objective function is defined in the domain of the wavenumber spectrum in which the operator must be accurate and the constraint function is defined in the remaining part of the wavenumber domain. The objective function we use is defined as the summation of the squared amplitude and phase errors over all wavenumbers in the domain of interest. The constraint function is designed to suppress the larger wavenumber to a value smaller than 1.0 in order to obtain stable operators.

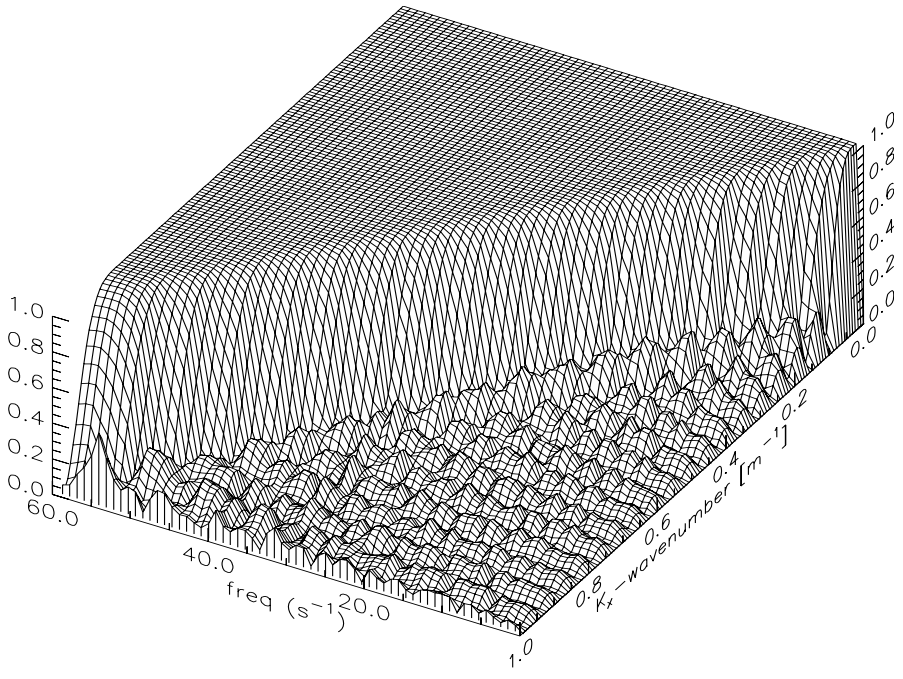

Figure A.6: *K_x-ω representation of the weighted least squares operators (same parameters as before). The evanescent region is stable and the propagating region is accurate for all frequencies.*

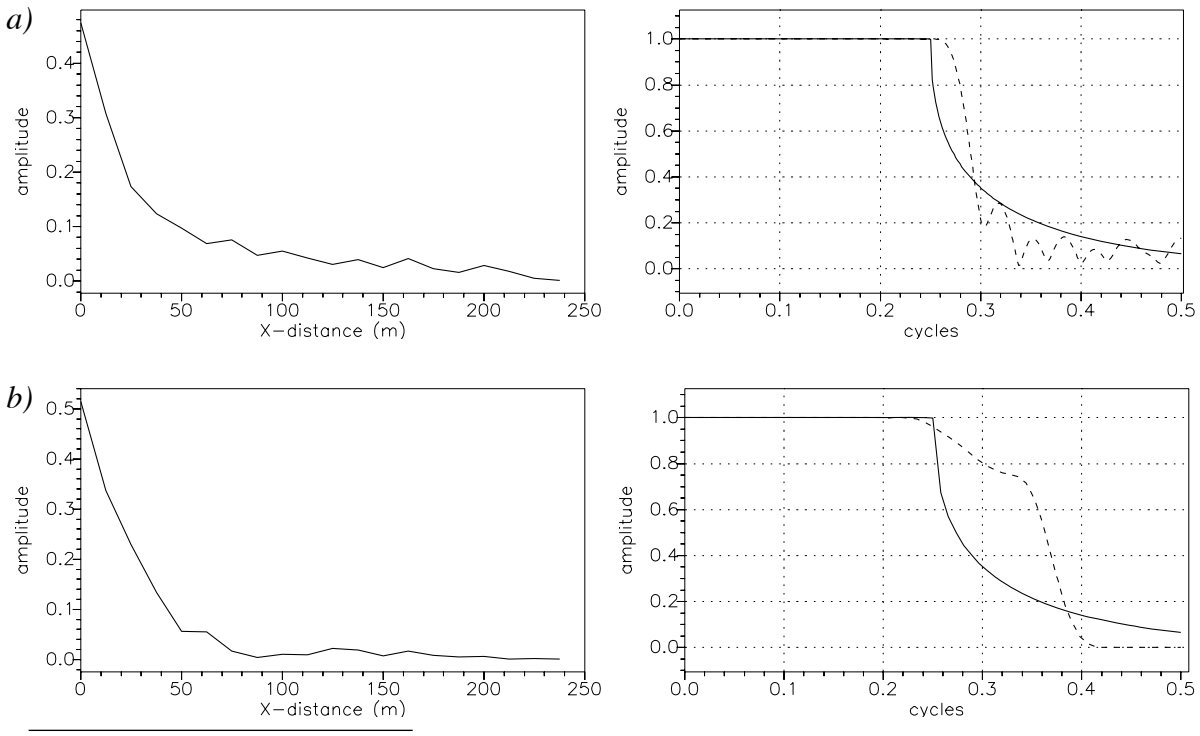

Figure A.7: *Non-linear optimization with FSQP (a) and NAG (b). Both methods give excellent results in the propagating region. The different behavior in the evanescent region is also due to a different initial guess.*

Two different non-linear optimization routines are used; the FSQP routine written by Tits and Zhou (1993) and a NAG lib routine. The initial guess, which must be provided, is for both methods the truncated spatial operator. If the methods fail to find a solution with the provided initial guess the smoothed phase or the weighted least squares solution is taken as initial guess. The results are shown in Figure A.7 a for the FSQP routine and for the NAG routine in Figure A.7 b. Because the NAG method does not converge when 512 wavenumber samples are chosen the number of samples is reduced to 128. Both methods give stable and accurate results, the optimized result with the NAG routine is obtained with the smoothed phase operator as initial guess. A disadvantage of the NAG method is that the computation time is long and it does not always find a solution. However, a slight change in the input parameters (for example by changing the maximum angle of interest) can give a correct solution. Due to these practical disadvantages we prefer the FSQP method.

Now that we have introduced five types of methods (Gaussian filtering, truncation, smoothed phase, weighted least squares and non-linear optimization) for obtaining extrapolation operators we can compare them with each other. The same parameters are used as before only this time with an operator length of 19 points to show the differences more pronounced. The results are shown in Figure A.8. The weighted least squares method is in the figures indicated by wlsq and the non-linear method is indicated by fsqp. From the spatial wavelet in Figure A.8a it is observed that the weighted least squares and the non-linear optimization procedure have relative high amplitude variations for the greater offsets. So the contribution from the off-center points is greater in the non-linear and the weighted least squares methods than in the other

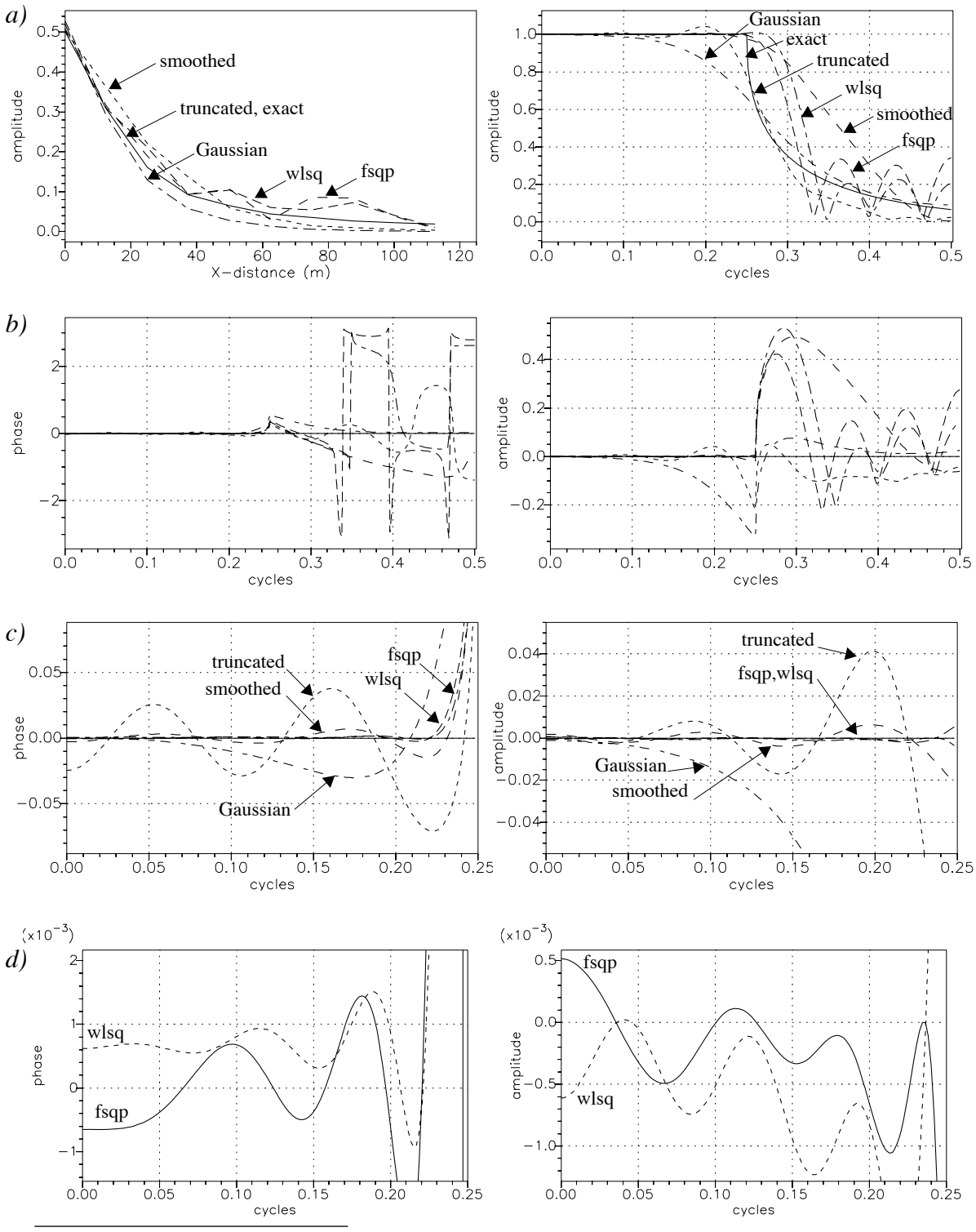

Figure A.8: *a) Different extrapolation operators in x (left) and its k_x-spectrum (right) of a 19 point spatial operator (wlsq denotes the weighted least squares method and fsqp denotes the non-linear method).*
b) Phase (left) and amplitude (right) errors for the operators shown in Figure A.8a.
c) Detailed view in the propagating region for the phase (left) and amplitude (right) errors.
d) Amplitude and phase errors for the weighted least squares and non-linear method.
For a detailed discussion of the different operators the reader is referred to the text.

methods. Application of these operators (with a long operator length) in inhomogeneous media can therefore give rise to artefacts in the extrapolation. The other spatial wavelets decays more 'smoothly' for the off-center points. In the wavenumber spectrum the differences between the operators can be interpreted more meaningful. The phase and amplitude errors of the operators are displayed in Figure A.8b and c. From the wavenumber spectrum we see that the Gaussian operator is already loosing amplitudes for small angles. The phase was also not correct, but as Nautiyal already pointed out we should subtract the phase at $k_x = 0$ from the result to obtain the correct phase (thus by using a shifted Gaussian). The truncated operator is not stable for all wavenumbers especially for the wavenumbers just before the point where the evanescent part starts the amplitude exceeds amplitude 1 significantly. The smoothed phase operator is in this area more stable and accurate than the truncated operator. The weighted optimized operator is stable and accurate for all wavenumbers. In the evanescent region the amplitude is larger than the other operators (but still smaller than 1). The phase errors are very small and the amplitude errors are smaller than 0.001. The non-linear optimized operator is as good as the weighted least squares operator but has a little different behaviour as shown is Figure A.8d. The weighted least squares solution has a negative error for most wavenumbers, thus is unconditionally stable within the domain of interest, while the non-linear method has also small positive errors.

In this section we have shown that there are several ways to obtain a spatial convolution operator. From the examples given above it can be concluded that the spatial bandwidth of a desired spatial convolution operator must, in the optimization procedure, be constrained to a *desired bandwidth*. To overcome exponentially amplifying of certain propagating wavenumbers in a recursive depth migration it must also have a *stable* behaviour. In the next section we will apply the operators in an explicit recursive migration scheme to observe the effects of different operators in a depth section. From the foregoing results we are not able to say something about the depth migrated result. It is interesting to see how the differences observed in Figure A.8 above can be found back in the depth section.

A.4 Recursive depth migration

In recursive depth migration lateral varying convolution operators are used to extrapolate seismic data through inhomogeneous media. The extrapolation operators in the x-ω domain are homogeneous operators for each grid point (x, z). Based on the frequency ω and the local velocity c in gridpoint (x, z) the extrapolation operator is computed, or in general read from an operator table which is computed in advance based on the frequency range of interest and the minimum and maximum velocity found in the macro model. Because of this assumption, the extrapolation depth step should be small, the operator length short and the extrapolation should be applied recursively. To obtain reliable extrapolation results the operators must be accurate and remain stable in the recursion scheme. For accuracy the k_x-ω spectrum of the spatial operators must be close to the exact k_x-ω spectrum of the phase shift operator in the specific band of interest. Stability requires that the amplitude of the spectrum is smaller or equal to 1. In the previous section it was shown that with these constraints it is possible to use different methods

to design the operators. In this section five different extrapolation operators are considered: the truncated, smoothed phase, gaussian tapered, non-linear (FSQP) and the weighted least squares operator.

Homogeneous shot record migration experiments are carried out in a medium with a velocity of 2000 m/s, a length of 2000 m and a depth of 1000 m with x and z intervals, $\Delta x = \Delta z = 10$ m. The zero offset trace in the shotrecord contains three Ricker wavelets at 0.3 s, 0.6 s and at 0.9 s (the other traces are filled with zero's). The source wavelet is sampled with 4 ms and has an amplitude spectrum up to 60 Hz. In Figure A.9 ten depth sections are shown for five different extrapolation operators and two different operator lengths. In Figure A.9a the results for the weighted optimization procedure are shown. The left-hand side picture gives a depth section with an operator length of 19 points designed to be accurate for angles up to 65 degrees. The right-hand side picture represents a depth section obtained with an operator length of 39 points and a maximum design angle of 85 degrees. The weight function used to obtain these results is the simple box function described earlier. The higher angles in the 19 point operator are not accurate and the steeper dips are attenuated, we will discuss this later. Note that the events observed in the depth images lie on concentric semicircles with centers at the origin. In Figure A.9b the smoothed phase operators are shown with the same constraints as in Figure A.9a. The result is stable but contains noise for the 85 degrees experiment and the higher angles in the 65 degrees experiment are less accurate than the optimized result. In the deepest event in the depth section of the 19 point result the cumulative error can be observed in the distorted semicircle. The truncated operator result in Figure A.9c is not stable for the 19 point operator. The 39 point operator is stable but the edge effects of the operator disturb the image strongly. Figure A.9d gives the result with the Gaussian taper. The migrated section has the smallest artefacts in it but the price is that the higher angles are strongly attenuated and in the 19 point operator result the deepest event is almost vanished. Finally in Figure A.9e the non-linear optimization result is shown. The result with the 19 point operator shows a good section even up to the highest angles, but there are also some artefacts at the higher angles. The non-linear 39 point operator gives a better result but it takes a very long time to compute the operator table.

In Table A.1 the computation times of the operator table for the different techniques for the migration experiments in Figure A.9 are given. The operator table which is calculated in

Operator type	39 points	19 points
Truncated	3.733 seconds	3.717 seconds
Gaussian Taper	3.333 seconds	3.283 seconds
Smoothed Phase	3.050 seconds	3.033 seconds
Weighted Least Squares	12.367 seconds	7.567 seconds
Non-linear (FSQP)	4457.483 seconds	968.616 seconds
Non-linear (NAG)	> 15,000 seconds	4295.416 seconds

Table A.1 *Computation time for operator table calculation on Convex C220.*

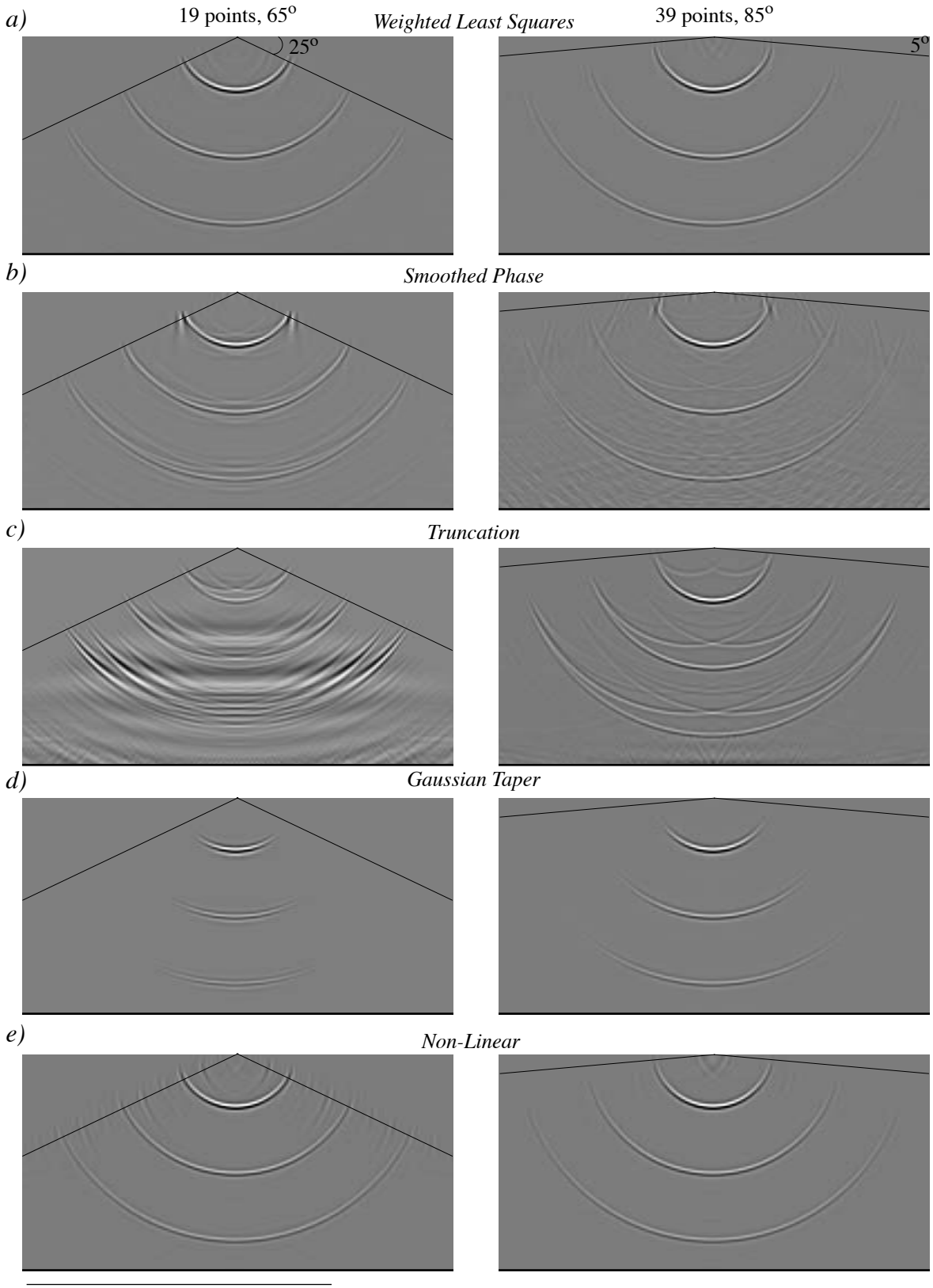

Figure A.9: *Impulse responses for five different extrapolation operators. The left picture shows the result for an operator with 19 points and a maximum design angle of 65° and the right picture shows an operator of 39 points with a maximum design angle of 85°.*
a) weighted least squares, b) smoothed phase, c) truncated, d) Gaussian tapered, e) non-linear optimized. Indicated are the regions for which the operators are designed to be accurate.

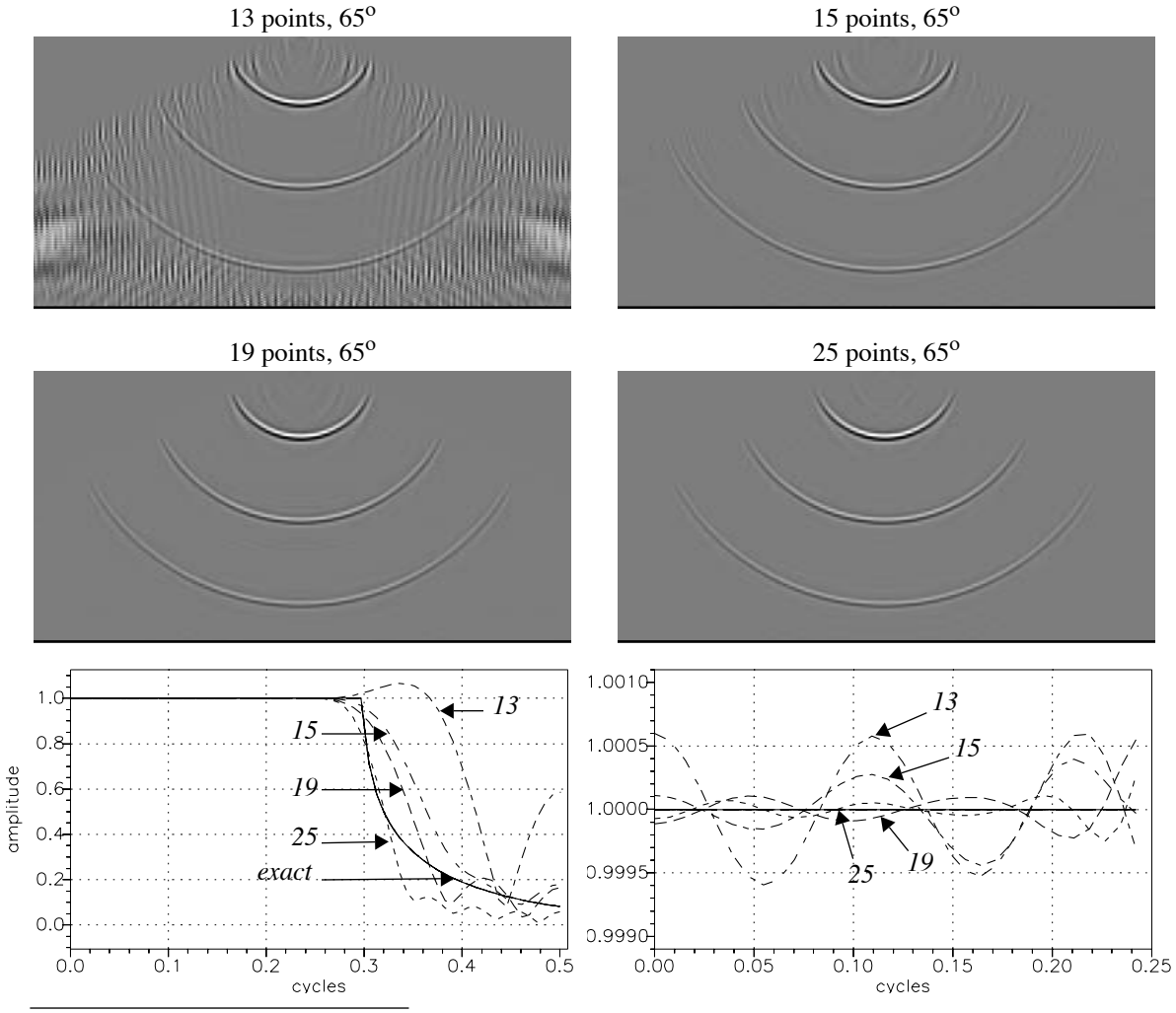

Figure A.10: *Depth sections obtained with different optimized operator lengths in the wlsq method with a fixed maximum design angle of 65°. Below are the wavenumber spectra given for a frequency of 30 Hz and a detailed view of the spectra in the propagating region. The artefacts which are observed in the depth section can be found back in the wavenumber spectrum of the operators.*

advance consists of 1441 operators. The truncated, Gaussian and smoothed phase operator calculation use the same amount of computation time, the weighted least squares method consumes 4 times more time. The two non-linear optimization methods takes a very long time to compute all operators. It is therefore not very efficient to compute the operator table with the non-linear optimization routines.

The possibilities and limitations of the weighted least squares procedure are illustrated with some simple examples. From a computational point of view the desired operator length must be as short as possible. To illustrate the influence of reducing the number of operator points the experiment of Figure A.9a is repeated for different operator lengths. The results are shown in Figure A.10. The 13 point operator is inaccurate and unstable for the steeper dips, the 15 point operator is stable but for steeper dips it is still inaccurate. This inaccuracy can be observed most clearly in the smallest semicircle. It is remarkable that the 15 point operator is so much better than the 13 point operator. The 19 point operator is both accurate and stable, the 25 point oper-

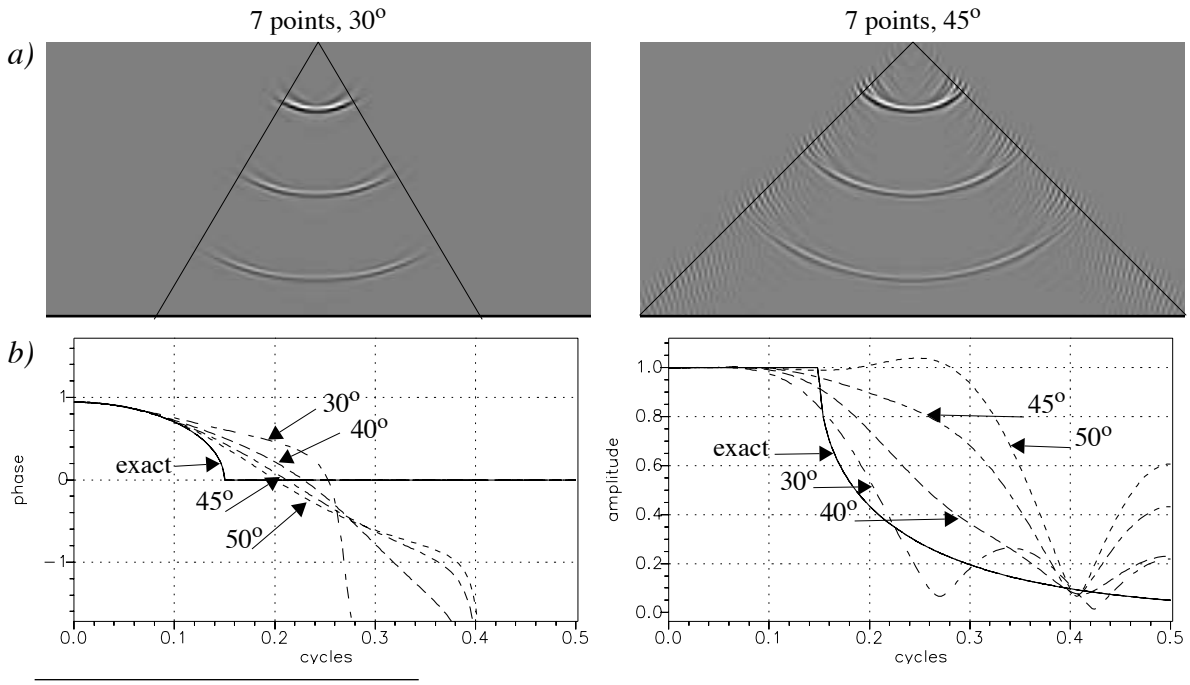

Figure A.11: *Using the weighted least squares method several maximum design angles are considered for a fixed operator length of 7 points:a)Left: depth section with a design angle of 30° Right: depth section with a design angle of 45° b) Amplitude and phase spectrum for a 7 point operator for different design angles at 30 Hz. Due to the behaviour of the operator in the evanescent region high frequency artefacts are observed in the depth section.*

ator is stable and even more accurate but this is hardly visible. From these migration results it is difficult to predict how an operator with a certain length behaves. The only practical rule is that a longer operator in a homogeneous medium will always be more accurate and stable than a shorter operator. The wavenumber spectra, for a representing frequency, of the different operators gives more information about the accuracy and stability of the operator. It is remarkable that the unstable 13 points operator has a stable behaviour in the propagating region and is unstable for the evanescent region. This is also observed in the migrated section which contains high frequency artefacts. In the wavenumber spectra it is also observed that more operator points in the spatial domain will give smaller amplitude errors in the propagating region.

When the maximum angle of interest is reduced the operator length can also be reduced to obtain the same result within a shorter computation time. In the limit a 1 point operator is sufficient to extrapolate a plane wave. In Figure A.11a the wavenumber and phase spectrum is shown for a 7 point operator for different maximum design angles. The parameters are the same as before, the frequency shown in Figure A.11a is 30 Hz. In the amplitude spectrum an interesting property is observed; for higher design angles the operator has a bigger amplitude at the evanescent region, for the 50° operator even bigger than 1. This property is also observed in the right-hand side depth section in Figure A.11b. The 45° depth section is inaccurate for the higher angles. For the 30° operator the depth section is more accurate and the higher angles of propagation are attenuated. With these simple experiments it is shown that an operator cannot be both short and accurate for steep dips. In designing a short operator the higher angles must be attenuated to overcome steep dip distortion.

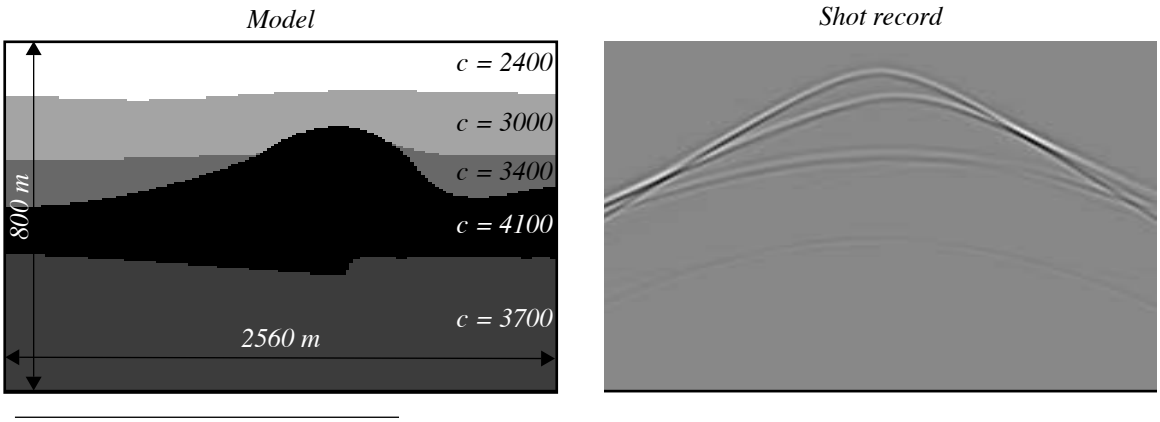

Figure A.12: *Inhomogeneous model and a shot record at the middle of the model.*

To illustrate the effects of the different operators in an inhomogeneous medium the model shown in Figure A.12 is used. The model consisted of 160 lateral positions, sampled with 16m, and 161 depth levels, sampled with 5m. The data consists of 160 traces of 256 samples, sampling interval 4 ms. First we will perform the migration of one shot record for the five different operators and two different operator lengths. Next, we will do the same for an areal shot record migration, defining a horizontal plane wave at target level. The target level in this experiment is the fault structure below the dome.

In Figure A.13 the migrated results are shown for operators with an operator length of 19 points, 128 wavenumber samples and a maximum design angle of 65 degrees. A 19 point operator is chosen because in the homogeneous experiments we saw that for the optimized operators this gives already good results. The truncated operator shows the most unfavorable result, it contains a lot of high-angle artefacts and smears out lateral inhomogeneous layers through the migration result. The Gaussian tapered operator attenuates too much significant information and is therefore not useful for accurate results at greater depths. The smoothed phase operator handles the higher angles not very good, which give rise to the smearing of data in the pictures. The non-linear operator gives results which are nearly as good as the weighted least squares optimization procedure, some artefacts are visible above the fault structure.

In Figure A.14 the results are shown for a 7 point operator which is designed to be accurate for angles up to 40 degrees. This limitation in the maximum angle is due to the fact that the non-linear procedure is not stable for angles greater than 40 degrees. The weighted least squares operator gives the best result. All structures are positioned at their proper positions. The deepest event in the smoothed phase operator is not good and the Gaussian tapered operator does not even show this deepest event. The non-linear operator has more artefacts but the boundaries of the reflectors are positioned correct. The truncated operator shows more artefacts than reflections.

Finally an example with controlled illumination is given (DELPHI, Vol. III, Chapter 6). The illumination is defined for a plane wave at target level (just below the dome structure). Because of the angle of the illuminating wave field at target level (0°) and the moderate contrasts and

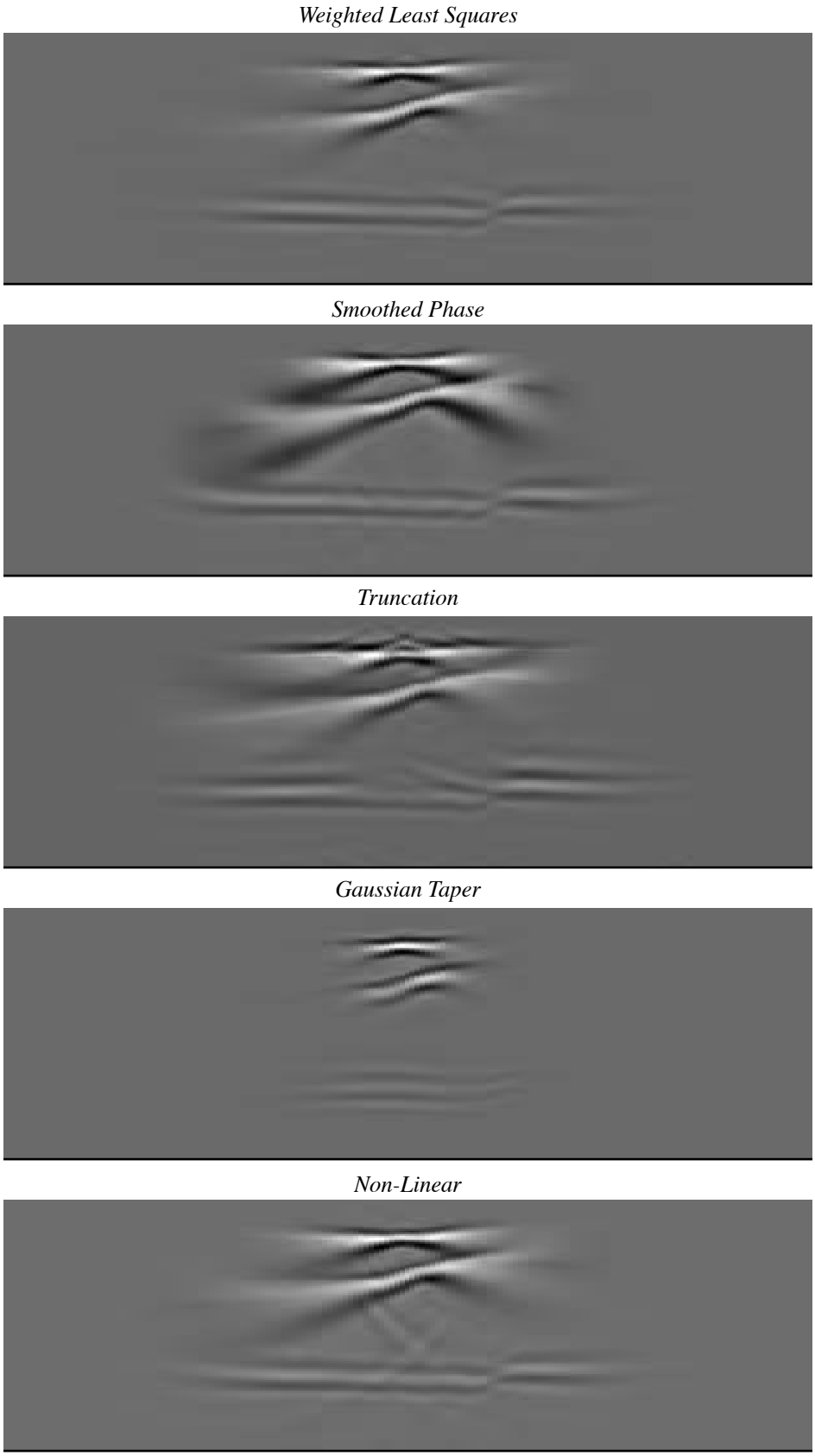

Figure A.13: *Single shot record migration results for the inhomogeneous model shown in Figure A.12 with five different operators with an operator length of 19 points and a maximum angle of 65 degrees. For the deepest event the difference between the different operators can be observed most clear.*

Weighted Least Squares

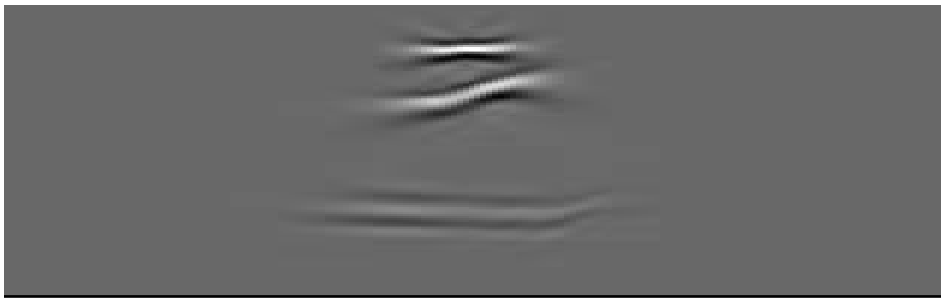

Smoothed Phase

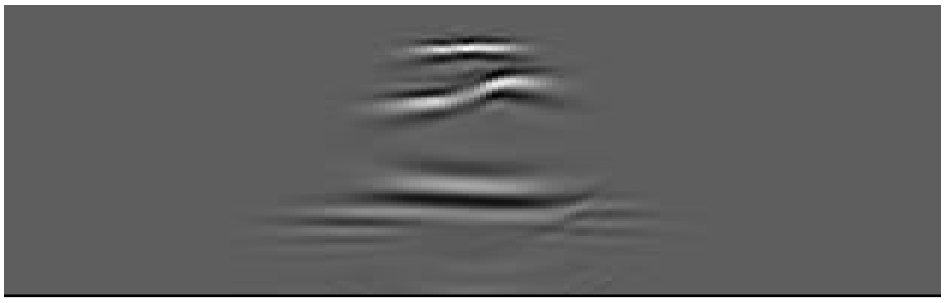

Truncation

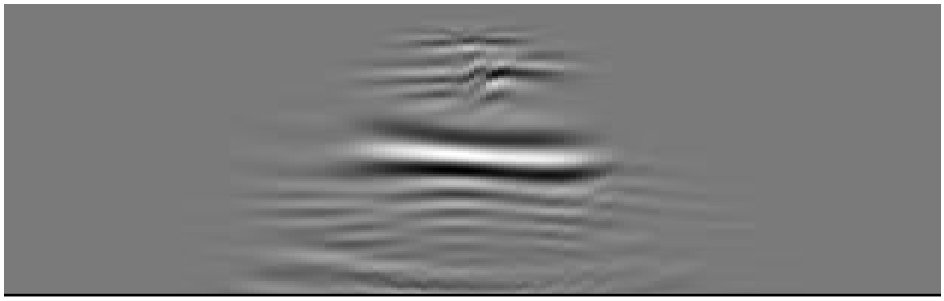

Gaussian Taper

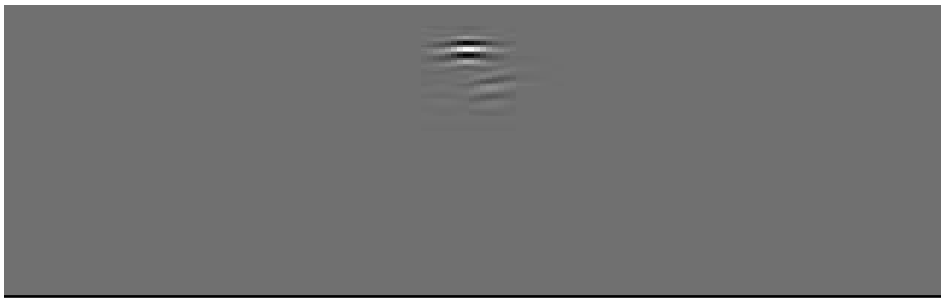

Non-Linear

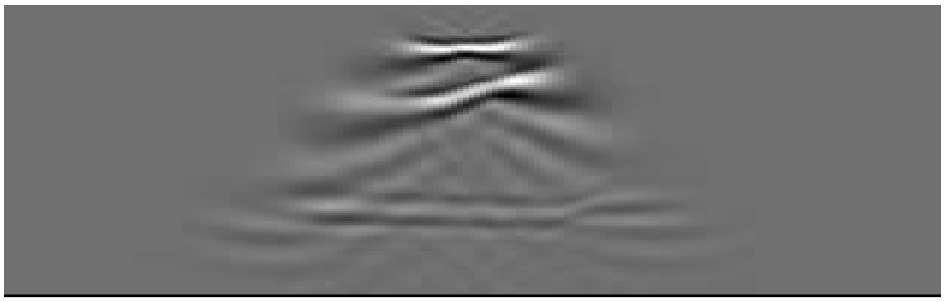

Figure A.14: *Single shot record migration results for the inhomogeneous model shown in Figure A.12 with five different operators with an operator length of 7 points and a maximum angle of 40 degrees. At the deepest event the differences are observed most clear.*

structures in the model, the range of angles of interest in this example is restricted to small angles. Hence, the extrapolation operators can be chosen very short without disturbing the migrated result. The results for different operators are shown in Figure A.15. The operators used in Figure A.15 have all 7 points and are accurate up to 40 degrees. The smoothed phase and the truncated operator gives artefacts and phase errors for the deepest event. The weighted least squares and the non-linear optimization procedures give good results. The Gaussian tapered operator attenuates the deepest event and the higher angles too strong.

A.5 Conclusions and future plans

The operators obtained with the weighted least square optimization procedure are economic, stable and accurate. Reducing the operator length will decrease the computation time, but for very short operators the steep dip will become inaccurate and unstable. Comparing the weighted least square operators with the computationally intensive non-linear optimized operators (see Table A.1), it may be concluded that only a small difference occurs at the high angles: the weighted least squares operator decays a little in amplitude while the non-linear operators keep the amplitude correct (although they give rise to small artefacts at the high angles). In the DELPHI project we have chosen for the weighted least squares method to compute the operator table, because of its stable and accurate behaviour for a broad range of operators and the relatively small computation time.

The weight function used in the optimization procedure can also be optimized in order to give the spatial operator an even more controlled behavior. This optimization of the weight function is a topic for future research. The length of the optimized operator is for a certain error a function of the wavenumber. In calculating the table of operators this length dependency could be taken into account to arrive at an even more efficient extrapolation. At the moment we are also investigating a similar optimization process for 3D operators.

A.6 References

Berkhout, A.J., 1985, *Applied seismic wave theory*: Elsevier Science Publishers.

Blacquière, G., 1989, *3D wave field extrapolation in seismic depth migration*, Ph.D. thesis, Delft University of Technology.

DELPHI, 1992, Volume III, Chapter 6, *Target oriented processing based on controlled illumination*, 163 - 204, Delft University of Technology.

DELPHI, 1993, Volume IV, Appendix D, *Short operators by generalized Fourier transformation*, 433 - 454, Delft University of Technology.

Hale, D., 1991, *Stable explicit extrapolation of seismic wave fields:* Geophysics **56**, 1770-1777.

Weighted Least Squares

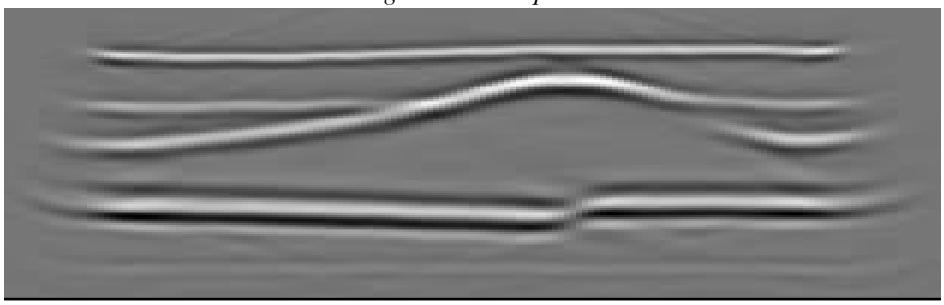

Smoothed Phase

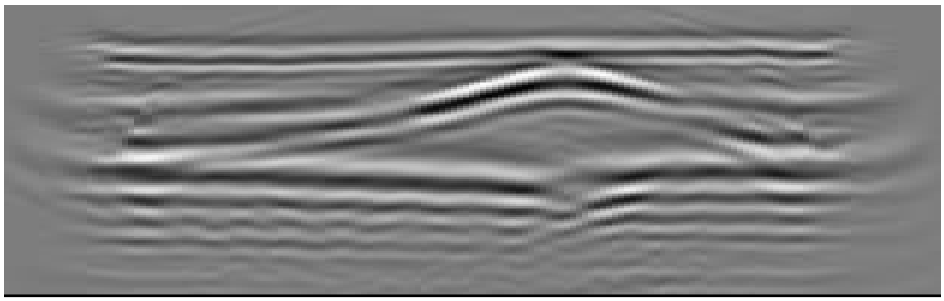

Truncation

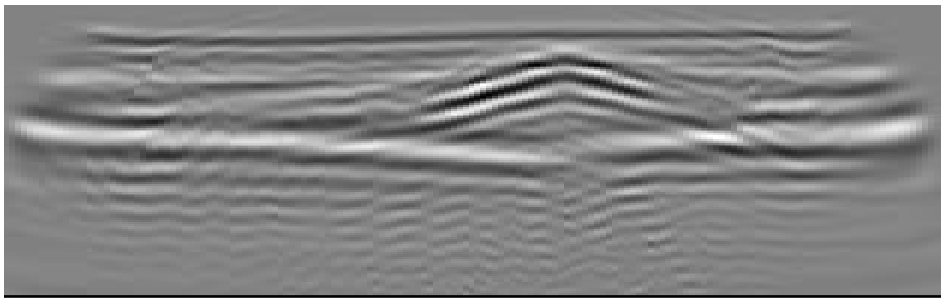

Gaussian Taper

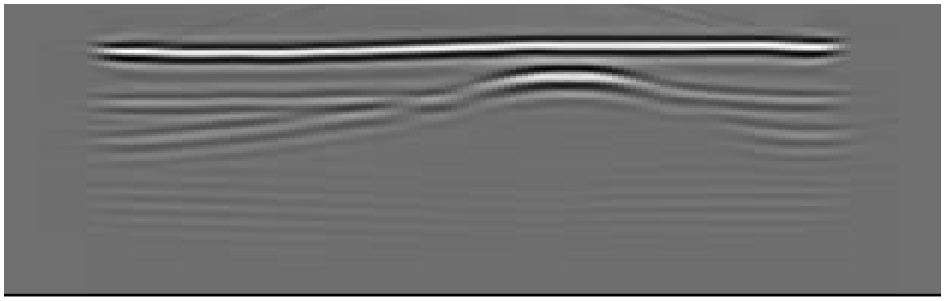

Non-Linear

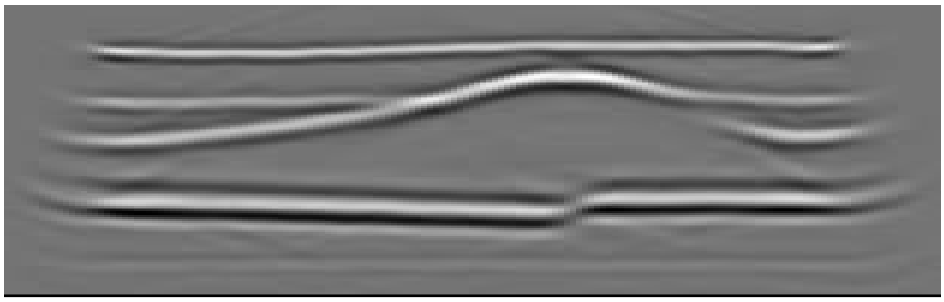

Figure A.15: *Controlled illumination for a plane wave at target depth for different operators with an operator length of 7 points and a maximum angle of 40 degrees. Note the very good results for the weighted least squares and the non-linear method considering this very short operator.*

Holberg, O., 1988, *Towards optimum one-way wave propagation:* Geophys. Prosp. **36**, 99-114.

Nautiyal, A., Gray, S.H., Whitmore, N.D. and Garing, J.D., 1993, *Stability versus accuracy for an explicit wavefield extrapolation operator:* Geophysics **58**, 277-283.

Tits, A.L. and Zhou, L.H., 1993, *User's guide for FSQP Version 3.3b: A Fortran code for solving Constrained Nonlinear (Minimax) Optimization Problems, Generating Iterates Satisfying All Inequality and Linear Constraints*: personal notes.

Wapenaar, C.P.A. and Berkhout, A.J., 1989, *Elastic wave field extrapolation, Redatuming of single-and multi-component seismic data*: Elsevier Science Publishers.